

Article

Synergistic Lubrication and Antioxidation Efficacies of Graphene Oxide and Fullerenol as Biological Lubricant Additives for Artificial Joints

Qian Wu ^{1,†} , Honglin Li ^{2,†}, Liangbin Wu ¹, Zihan Bo ¹, Changge Wang ¹, Lei Cheng ¹, Chao Wang ¹, Chengjun Peng ^{1,3}, Chuanrun Li ¹, Xianguo Hu ⁴ , Chuan Li ^{2,*} and Bo Wu ^{1,*} 

¹ Pharmaceutical Engineering Technology Research Center, School of Pharmacy, Anhui University of Chinese Medicine, Hefei 230012, China

² Key Laboratory of Resource Comprehensive Utilization, School of Chemistry and Material Engineering, Chaohu University, Hefei 238014, China

³ Anhui Province Key Laboratory of Pharmaceutical Preparation Technology and Application, Hefei 230012, China

⁴ School of Mechanical Engineering, Hefei University of Technology, Hefei 230009, China

* Correspondence: 053039@chu.edu.cn (C.L.); wubo@ahctm.edu.cn (B.W.)

† These authors contributed equally to this work.

Abstract: The service life of artificial joints has gradually failed to meet the needs of patients. Herein, the synergistic lubrication and antioxidant efficacies of graphene oxide (GO) and fullerenol (Fol) as biological lubricant additives for artificial joints were investigated. The lubrication mechanisms of biological lubricant containing GO and Fol at the friction interface of artificial joints were then revealed. Tribological tests showed that the average friction coefficients of Al₂O₃-Ti6Al4V pairs and Ti6Al4V-UHMWPE pairs for artificial joints could be reduced by 30% and 22%, respectively, when GO and Fol were used as biological lubricant additives simultaneously. The lubrication mechanism showed that some incommensurate sliding contact surfaces could be formed between the GO nanosheets and spherical Fol at the interface, which reduced the interaction forces of friction pairs. The maximum scavenging rates of •OH and DPPH free radicals by the biological lubricant containing GO and Fol were 35% and 45%, respectively, showing a good antioxidant efficacy of the biological lubricant. This can be attributed to the GO and Fol scavenging free radicals through electron transfer and hydrogen transfer. This study provides a theoretical basis for the development and application of carbon nanomaterials as biological lubricant additives for artificial joints in the future.

Keywords: biological lubrication additives; artificial joint; carbon nanomaterials; lubrication; antioxidation



Citation: Wu, Q.; Li, H.; Wu, L.; Bo, Z.; Wang, C.; Cheng, L.; Wang, C.; Peng, C.; Li, C.; Hu, X.; et al. Synergistic Lubrication and Antioxidation Efficacies of Graphene Oxide and Fullerenol as Biological Lubricant Additives for Artificial Joints. *Lubricants* **2023**, *11*, 11. <https://doi.org/10.3390/lubricants11010011>

Received: 30 November 2022

Revised: 24 December 2022

Accepted: 27 December 2022

Published: 30 December 2022



Copyright: © 2022 by the authors. Licensee MDPI, Basel, Switzerland. This article is an open access article distributed under the terms and conditions of the Creative Commons Attribution (CC BY) license (<https://creativecommons.org/licenses/by/4.0/>).

1. Introduction

The incidence of the human joint system is rapidly increasing with age, genetics, obesity and other factors [1]. It is difficult for bone joints to heal after injury or pathological changes. Artificial joint replacement, as a safe and effective method for the treatment of advanced joint diseases, has been widely implemented all over the world. It is described as the process of a prosthetic joint component made of metal, ceramic or polymer replacing a damaged natural bone joint [2]. However, the prosthetic material is always in a state of direct contact friction due to the absence of synovial fluid secreted by the synovial membrane and cartilage tissue in the patient's natural joint system [3]. This leads to the wear of the prosthetic material inevitably and reduces the service life of the artificial joint greatly. In addition, metal and other prosthetic materials produce some wear debris in the process of friction [2]. These wear debris induce the production of reactive oxygen species (ROS) in the human tissue around the prosthesis and lead to a series of adverse biological reactions such as osteolysis, resulting in the failure of the artificial joint due to

aseptic loosening [4–6]. Based on available clinical data, the safe service life of artificial joints in the human body is only ten to fifteen years [7]. With the reality of younger patients presenting with osteoarthritis, the current service life of artificial joints obviously cannot meet the actual needs of patients. Therefore, it is necessary to improve the lubrication of the artificial joint system and inhibit the wear of prosthetic materials to prolong the service life of artificial joints.

Extracorporeal injection of joint biological lubricant is the traditional way to improve the lubrication property of artificial joint surfaces. At present, the joint biological lubricant used in clinical environments is hyaluronic acid (HA) [8]. Studies have found that 30% to 40% of a gait cycle is in a state of fluid lubrication during normal activity of joints, and most of the rest time is in a state of boundary lubrication. HA can play the role of fluid lubrication at the natural cartilage interface by changing the viscosity of synovial fluid. However, HA molecules break and lose their good lubrication effect under the condition of boundary lubrication [9,10]. Consequently, HA cannot fully guarantee that the joint interface is in a good lubrication condition under various complex motion conditions. In addition, as an injection lubricant, exogenous HA is hydrolyzed in the artificial joint system and excreted from the body [11,12]; thus, it cannot play a long-term lubrication role in the interface of joint prostheses. Therefore, the development of a lubricant with a stable lubrication effect under a boundary lubrication condition is of great significance to improve the service life of artificial joints.

In recent years, graphene oxide (GO) with a lamellar structure and fullerene (Fol) with a spherical structure as two typical representatives of carbon-based nanomaterials have attracted wide attention in the field of biological tribology due to their excellent physical and chemical properties and biocompatibility [13]. Researchers found that GO can reduce effectively friction and wear at the friction interface under a boundary lubrication condition by forming protective tribo-films and preventing the direct contact of the microconvex body [14–17]. Liu et al. reported that a water-soluble nanoparticle Fol as the lubrication additive could improve the friction performance and reduce the wear area significantly [18]. Chen et al. found that Fol could transform sliding friction into rolling friction during the friction process, reducing the friction coefficient and wear significantly [19]. More interestingly, researchers also found that GO and Fol have efficient free radical scavenging capabilities [20,21]. In particular, Fol has an antioxidant capacity hundreds of times higher than that of other antioxidants and acts as a free radical sponge in disease states associated with ROS overproduction [22–24].

These studies inspire us to use GO and Fol as biological lubrication additives for artificial joints at the same time. We hope that they can play a lubrication role at the interface of artificial joints, on the one hand, and play an antioxidant role in scavenging ROS in the body, on the other hand. In this way, the problems of wear and ROS increase in artificial joints can be solved simultaneously from two aspects, and the service life of artificial joints in the body can be prolonged as much as possible. In this study, the lubrication properties of GO and Fol at the interface of different artificial joint friction pairs were firstly investigated, and then the antioxidation properties of GO and Fol in scavenging reactive oxygen free radicals were evaluated. Finally, the lubrication and antioxidation mechanisms of GO and Fol were revealed. This study provides an important theoretical basis for the development and application of GO and Fol as biological lubrication additives for artificial joints in the future.

2. Materials and Methods

2.1. Materials and Reagents

GO was purchased from Nanjing XFNANO Materials Tech Co., Ltd. (Nanjing, China) Fol was purchased from Suzhou Dade Carbon Nanotechnology Co., Ltd. (Suzhou, China) 2, 2-diphenyl-1-picrylhydrazyl (DPPH), anhydrous ethanol, salicylic acid, ferrous sulfate (FeSO_4) and hydrogen peroxide (H_2O_2) were all purchased from Sinopharm Chemical Reagent Co., Ltd. (Shanghai, China) All reagents used were of analytical grade.

2.2. Preparation and Characterization of Biological Lubrication Additives

According to the mass ratio of 0.1 wt%, GO and Fol were added to ultrapure water in different proportions and ultrasonically dispersed for 60 min. Samples of the biological lubricant containing different proportions of GO and Fol additives were then obtained. Schematic diagram of experimental process was shown in Figure 1.

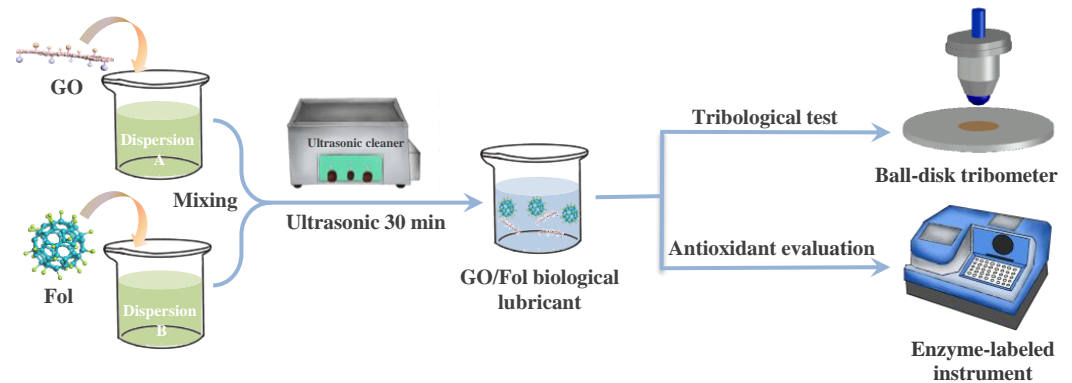


Figure 1. Schematic diagram of experimental process.

The morphology of the biological lubrication additives was studied by transmission electron microscopy (TEM, JEM-2100F, JEOL Ltd., Akishima-shi, Tokyo, Japan). The molecular structures of the biological lubrication additives were characterized by Fourier transform infrared spectroscopy (FTIR, Nicolet 6700, Thermo Fisher Scientific, Waltham, MA, USA). The accuracy of the FTIR was higher than 0.01 cm^{-1} and the resolution of the FTIR was higher than 0.09 cm^{-1} .

2.3. Dispersion Stability of Biological Lubrication Additives

The dispersion stability of different ratios of GO and Fol additives in biological lubricant was analyzed by an ultraviolet–visible spectrophotometer (UV-VIS, UV-8000, Shanghai Metash Instruments Co., Ltd., Shanghai, China). In general, the smaller the change in absorbance with time, the better the stability of GO and Fol dispersion in water [25]. The absorbance curves of biological lubrication additives GO, Fol, GO/Fol = 1/1, GO/Fol = 1/2 and GO/Fol = 2/1 in the wavelength range from 200 nm to 500 nm are shown in Figure 2a, and the changes in absorbance under the maximum absorption wavelength ($\lambda_{\text{max}} = 228\text{ nm}$) with storage time are shown in Figure 2b–f. It can be clearly seen from Figure 2 that the absorbance of all biological lubrication additives remains almost constant for 8 days, and there is no obvious stratification in the photographs of lubricant samples. This indicates that all GO and Fol additives have excellent dispersion stability as biological lubricants.

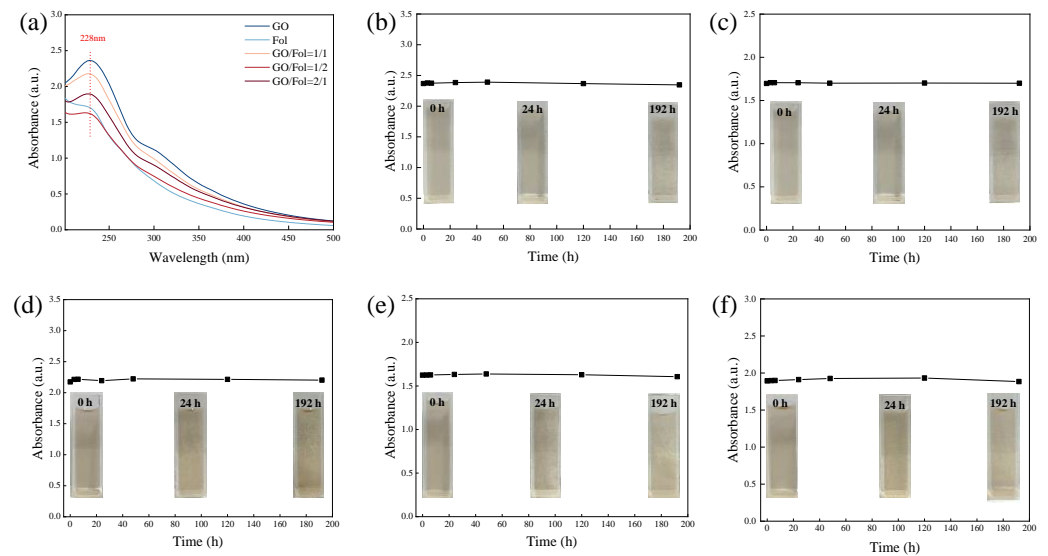


Figure 2. (a) The absorbance curves of biological lubrication additives GO, Fol, GO/Fol = 1/1, GO/Fol = 1/2 and GO/Fol = 2/1; changes in absorbance and photographs of biological lubrication additives (b) GO, (c) Fol, (d) GO/Fol = 1/1, (e) GO/Fol = 1/2 and (f) GO/Fol = 2/1 for different storage times.

2.4. Tribological Tests

Tribological tests were performed on a reciprocating ball–disk tribometer (CFT-I, Lanzhou Zhongkekaihua Technology Development Co., Ltd., Lanzhou, China). Before the tribological test, the ball and disk were cleaned ultrasonically for 30 min, and then the lubricant was dripped onto the ball–disk contact area. The stroke was set to 5 mm, the time was set to 30 min, the speed was set to 180 r/min, and the load was set to 1.5 N. Control experiments were performed on water without nanomaterials. Considering that metal, ceramic and polymer materials are widely used in existing artificial joints, we used two kinds of ball–disk friction pairs with different materials in this study. The materials used for the ball (Φ 6 mm) and disk (28 mm \times 28 mm \times 2.65 mm) are shown in Table 1. The friction coefficient (COF) was monitored in real time by the software provided with the tribometer, and the three-dimensional morphology of the wear tracks on the lower disk was photographed by a 3D laser scanning microscope (LSM, VK-X100, Keyence, Osaka, Japan). The chemical composition of the tribo-films on the wear surface was analyzed by Raman spectroscopy.

Table 1. Frictional pair materials.

Frictional Pair	Ball	Disk
Frictional pair 1	Al ₂ O ₃ (R _a , 3 μ m)	Ti6Al4V (R _a , 1 μ m)
Frictional pair 2	Ti6Al4V (R _a , 3 μ m)	Ultra-high-molecular-weight polyethylene (UHMWPE) (R _a , 1 μ m)

2.5. Antioxidant Activity

2.5.1. DPPH Free Radical Scavenging Activity

The above-mentioned biological lubrication additives were diluted in different proportions to obtain sample solutions with concentrations of 0.05 mg/mL and 0.1 mg/mL. The DPPH was prepared with anhydrous ethanol to 0.1 mmol/L. Then, 100 μ L of the sample solution and 100 μ L of the DPPH solution were added to a 96-well plate and then left in the dark for 30 min. The absorbance at 517 nm was recorded with an enzyme-labeled instru-

ment (Multiskan Spectrum, Thermo Fisher Scientific, Waltham, MA, USA). The inhibition rate (%) of DPPH free radical was calculated by the following Equation (1):

$$\text{DPPH free radical scavenging activity (\%)} = \frac{A_i - (A_x - A_{x0})}{A_i} \times 100\% \quad (1)$$

where A_i is the absorbance of ultrapure water instead of samples, A_x is the absorbance of added samples, and A_{x0} is the absorbance of anhydrous ethanol instead of DPPH solution.

2.5.2. Hydroxyl Free Radical Scavenging Activity

The scavenging ability of biological lubrication additives for hydroxyl radical was determined by the salicylic acid method. The above-mentioned biological lubrication additives were diluted in different proportions to obtain sample solutions with concentrations of 0.05 mg/mL and 0.1 mg/mL. A total of 50 μL of sample solution, 50 μL of 9.0 mM salicylic acid–ethanol solution, 50 μL of 9.0 mM FeSO_4 solution and 50 μL of 9 mM H_2O_2 solution were added to the 96-well plate. After incubation at 37 $^\circ\text{C}$ for 30 min, the absorbance at 510 nm was recorded with an enzyme-labeled instrument. The scavenging activity (%) of hydroxyl radical was calculated by the following Equation (2):

$$\text{Hydroxyl radical scavenging activity (\%)} = \frac{B_i - (B_x - B_{x0})}{B_i} \times 100\% \quad (2)$$

where B_i is the absorbance of ultrapure water instead of samples, B_x is the absorbance of added samples, and B_{x0} is the absorbance of ultrapure water instead of H_2O_2 solution.

3. Results and Discussion

3.1. Characterization

The microstructures of GO, Fol and GO/Fol were studied by transmission electron microscopy, as shown in Figure 3a–c. The morphology of GO showed an obvious ultra-thin nanosheet shape with some folds related to oxidation degree [26]. Spherical constructions with larger sizes can be easily found in Figure 3b due to the fact that Fol nanoparticles are easily agglomerated to form spherical clusters in water. However, smaller spherical Fol structures on the surface of GO were observed at the morphology of GO/Fol, shown in Figure 3c. This may be attributed to hydrogen bonding between GO and Fol, which inhibits the agglomeration of the Fol.

Figure 3d shows the functional groups of different biological lubrication additives. The peaks at about 1731 cm^{-1} , 1592 cm^{-1} , 1384 cm^{-1} , 1261 cm^{-1} and 1083 cm^{-1} belong to the characteristic absorption peaks of C=O stretching vibrations ($\nu\text{C=O}$), C=C stretching vibrations ($\nu\text{C=C}$), O–H in-plane deformation vibrations ($\delta\text{C-OH}$), C–O–C stretching vibrations ($\nu\text{C-O-C}$) and C–O stretching vibrations ($\nu\text{C-O}$), respectively. It can be seen from Figure 3d that Fol has the characteristic functional groups of $\nu\text{C=C}$, $\nu\text{C-O}$ and $\delta\text{C-OH}$, while GO and GO/Fol have the characteristic functional groups of $\nu\text{C=C}$, $\nu\text{C=O}$, $\nu\text{C-O}$, $\nu\text{C-O-C}$ and $\delta\text{C-OH}$. The above hydrophilic oxygenated functional groups give GO, Fol and GO/Fol excellent dispersion properties in water.

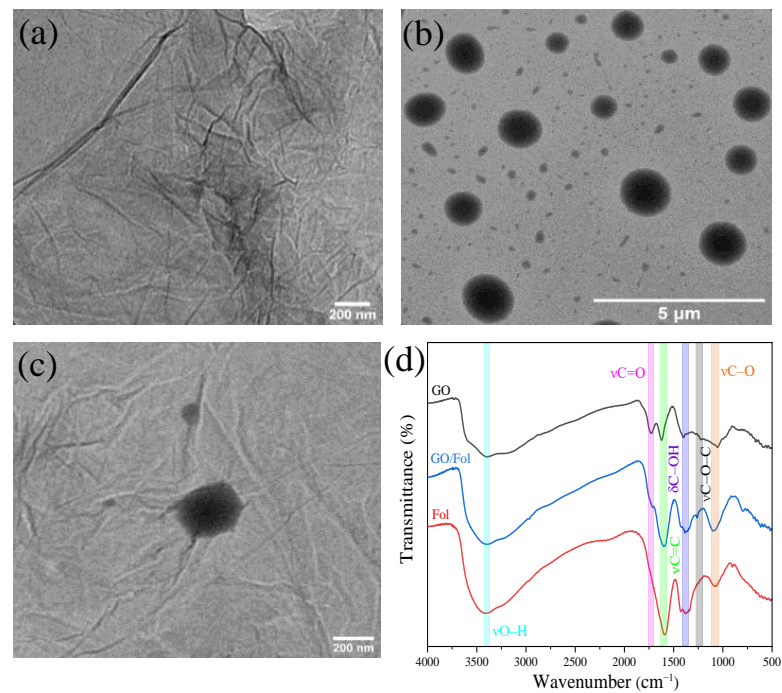


Figure 3. TEM images of (a) GO, (b) Fol and (c) GO/Fol; (d) FTIR spectra.

3.2. Evaluation of Lubrication Performance

3.2.1. Friction Reduction Properties of Biological Lubrication Additives

The friction reduction effect of GO/Fol biological lubrication additives with different proportions on two kinds of friction pairs was investigated on a reciprocating ball–disk tribometer. Figure 4a exhibits the relationship of the coefficient of friction (COF) of the pure water and the GO/Fol biological lubricant containing different proportions of additives on Al_2O_3 –Ti6Al4V pairs with the change in test time. In the half-hour friction test, the COF values of biological lubricants GO, Fol, GO/Fol = 1/1, GO/Fol = 1/2 and GO/Fol = 2/1 were almost lower than water as a lubricant, which indicated that GO/Fol biological lubrication additives provided friction reduction performance. The average coefficient of friction (AVCOF) values of the pure water and the GO/Fol biological lubricant containing different proportions of additives are shown in Figure 4b. The AVCOF of the GO/Fol = 2/1 biological lubricant could be reduced by 30% compared to pure water, which is obviously lower than biological lubricant containing only GO or Fol additives. The result indicates that GO and Fol can play a synergistic role to significantly improve the friction reduction performance of biological lubricants.

The COF curves of the pure water and the GO/Fol biological lubricant containing different proportions of additives on Ti6Al4V–UHMWPE pairs are shown in Figure 4c. It can be seen that the COF of water was obviously higher than that of GO, Fol, GO/Fol = 1/1, GO/Fol = 1/2 and GO/Fol = 2/1 biological lubricants and presented an increasing trend with the extension in test time. However, the COF of GO, GO/Fol = 1/1, GO/Fol = 1/2 and GO/Fol = 2/1 biological lubricants presented a decreasing trend with the extension in test time oppositely, which confirmed that GO/Fol biological lubrication additives also had excellent friction reduction performance on Ti6Al4V–UHMWPE pairs. The AVCOF values of the pure water and the GO/Fol biological lubricant containing different proportions of additives are shown in Figure 4d. The AVCOF values of all GO/Fol biological lubricants were lower than pure water under the same conditions. Compared to pure water, the AVCOF values of GO/Fol = 1/1, GO/Fol = 1/2 and GO/Fol = 2/1 biological lubricants decreased by 24%, 24% and 22%, respectively. Moreover, the AVCOF values of biological lubricants containing GO/Fol were significantly lower than those of biological lubricants containing only GO or Fol. This demonstrated that GO and Fol can also play a synergis-

tic role on the Ti6Al4V–UHMWPE pairs to significantly improve the friction reduction performance of biological lubricants.

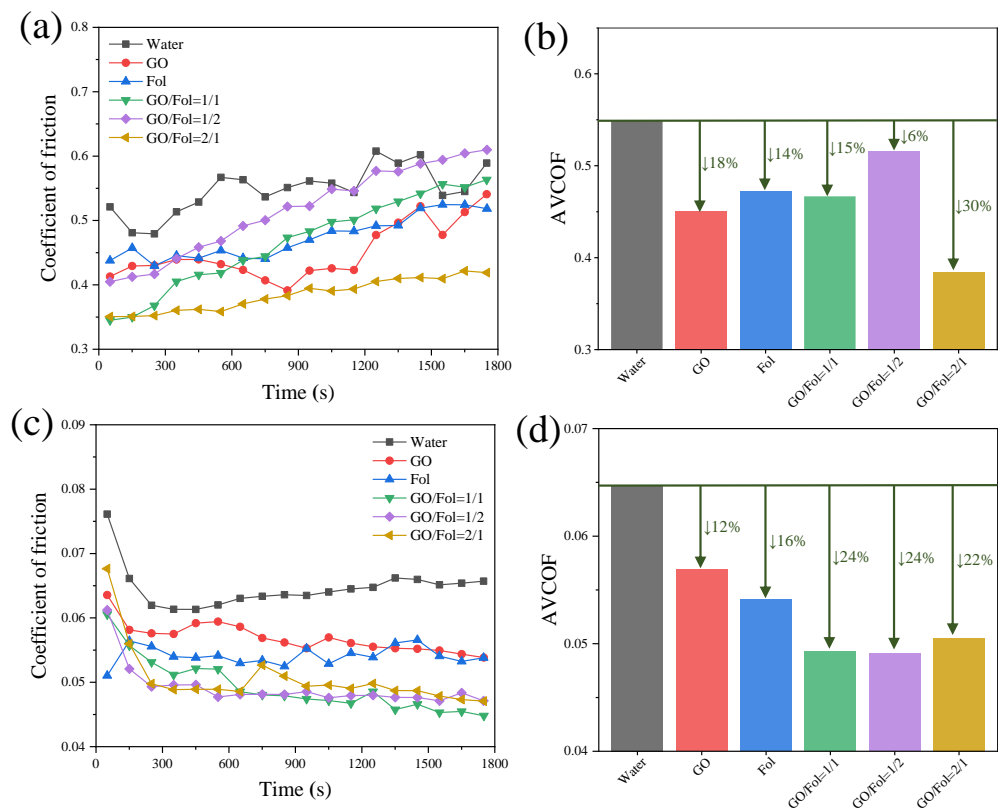


Figure 4. The coefficient of friction of the pure water and the GO/Fol biological lubricant containing different proportions of additives on (a) Al_2O_3 –Ti6Al4V pairs and (c) Ti6Al4V–UHMWPE pairs; the AVCOF of the pure water and the GO/F biological lubricant containing different proportions of additives on (b) Al_2O_3 –Ti6Al4V pairs and (d) Ti6Al4V–UHMWPE pairs.

3.2.2. Antiwear Properties of Biological Lubrication Additives

Microscopic images of wear scars on the Ti6Al4V disks lubricated by pure water and GO/Fol biological lubricants containing different proportions of additives are shown in Figure 5. When the pure water was used as lubricant, signs of deep grooves and serious scratches on the worn surface were observed. This may be caused by the long-term direct contact between the asperities on the surface of the upper and lower friction pairs, resulting in serious fatigue and abrasive wear. However, it can be clearly seen that the grooves became shallow and the wear track width decreased when the wear scar was lubricated by GO/Fol biological lubricants containing different proportions of additives as shown in Figure 5a. This indicated that the abrasive wear on the friction surface was inhibited by the GO/Fol biological lubrication additives to some extent. More specifically, the wear track width of biological lubricants containing both GO and Fol was obviously lower than that of biological lubricants containing only GO or Fol, which further confirmed the superior antiwear performance of GO/Fol biological lubricants owing to the synergistic effect of GO and Fol additives.

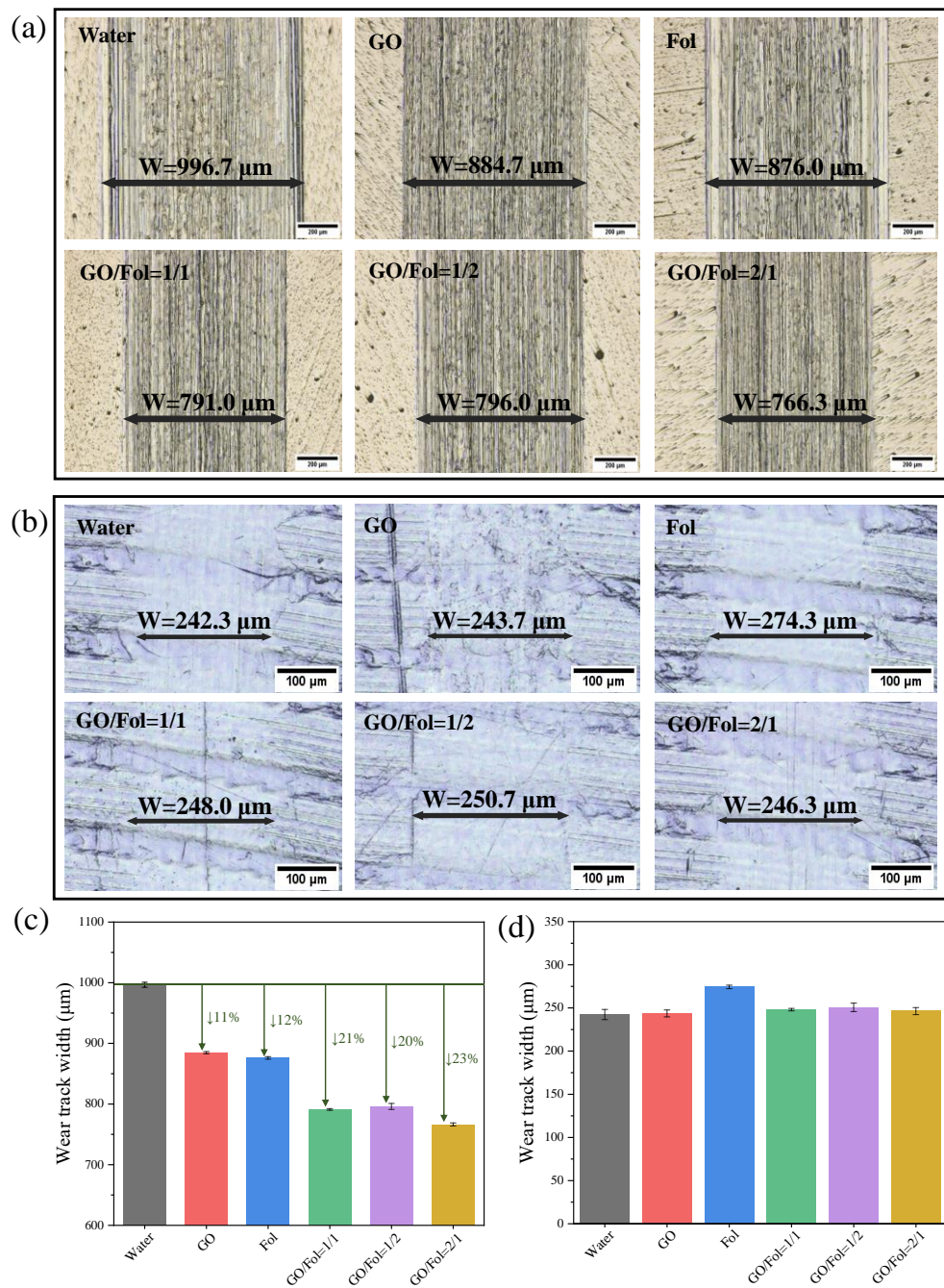


Figure 5. Microscopic images of wear scars on the (a) Ti6Al4V disks and (b) UHMWPE disks; the wear track width is indicated by the arrow line; the comparison of wear track width lubricated by pure water and GO/Fol biological lubricants containing different proportions of additives on the (c) Ti6Al4V disks and (d) UHMWPE disks.

Microscopic images of wear scars on the UHMWPE disks lubricated by pure water and GO/Fol biological lubricants containing different proportions of additives are shown in Figure 5b. The difference between the wear track width of biological lubricants and the pure water was small, indicating that the biological lubrication additives had little effect on the antiwear performance of pure water on the UHMWPE disks.

3.2.3. Composition Analysis of Wear Scars

The Raman spectra (Figure 6) and mappings (Figure 7) of the worn surfaces lubricated by pure water and different biological lubrication additives were measured to determine

the carbon microstructure and composition of wear scars. The Raman spectrum of the worn surface on the Ti6Al4V disks is exhibited in Figure 6a. The carbon characteristic peaks of D peak (1335 cm^{-1}) and G peak (1590 cm^{-1}) on the Raman spectra of the worn surface lubricated by biological lubricants containing GO additives can be seen, and these were the typical signals of SP^3 and SP^2 hybrid carbon structures, respectively [27]. However, the corresponding D peak and G peak were not identified on the wear scar lubricated by pure water. This shed light on the fact that GO could easily adhere to the worn surface and form protective tribo-films during friction [28]. Furthermore, no evident D peak or G peak could be observed in the Raman spectra of the worn surface lubricated by biological lubricants containing only Fol additives. This means that Fol was not easily adsorbed on the friction interface to form tribo-films. Interestingly, the I_D/I_G intensity ratio of the worn surface lubricated by biological lubricant containing GO/Fol additives was much lower than that of the worn surface lubricated by biological lubricants containing only GO additives, which indicated that more graphitized carbon-structured tribo-films could be formed on the worn surface lubricated by biological lubricants containing both GO and Fol additives. This phenomenon might be due to the fact that the spherical Fol could be interspersed and loaded onto the GO lamellae by hydrogen bonding, which enabled both the GO and Fol to enter the friction interface to form carbon tribo-films on the worn surface. Raman mappings (Figure 7) further confirmed that the distribution area of the carbon tribo-films on the worn surface of the Ti6Al4V disks lubricated by biological lubricants containing GO/Fol additives was obviously wider than that of biological lubricants containing only GO additives. The Raman spectra of the worn surface on the UHMWPE disks are shown in Figure 6b. The carbon characteristic peaks of D peak and G peak were not observed on the worn surface, indicating that the biological lubrication additives could not form tribo-films on the worn surface of the UHMWPE disks. This is in accordance with the above-founded result that the biological lubrication additives had little effect on the antiwear performance of pure water on the UHMWPE disks.

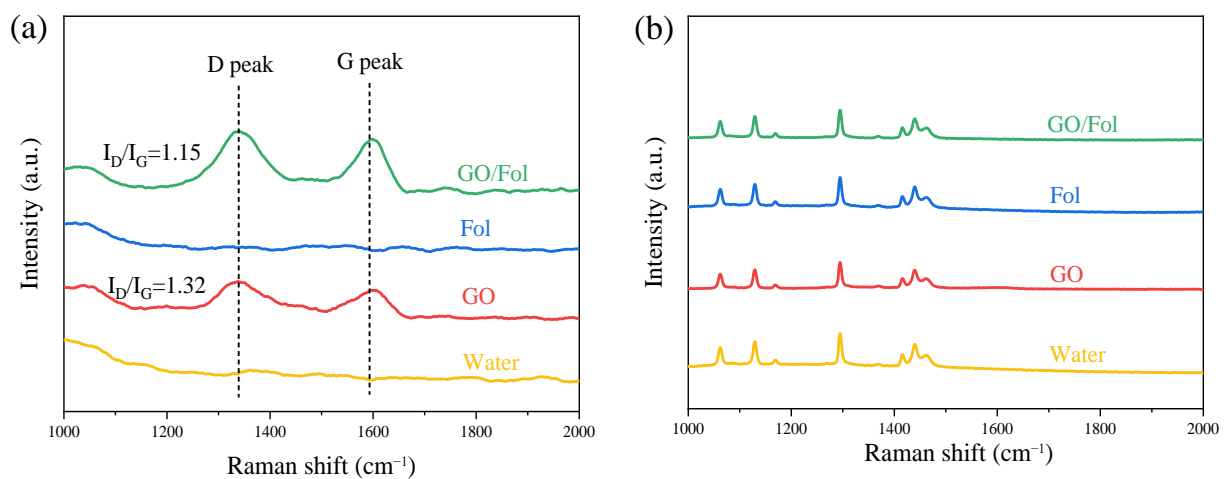


Figure 6. Raman spectra of the worn surfaces on the (a) Ti6Al4V disks and (b) UHMWPE disks lubricated by pure water and different biological lubrication additives.

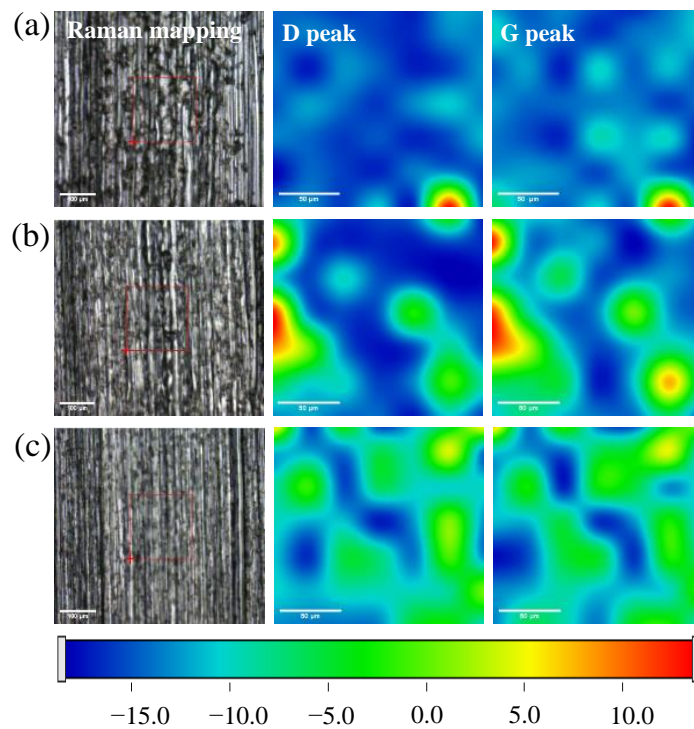


Figure 7. Raman mappings of the wear scars on the Ti6Al4V disks lubricated by (a) pure water, (b) biological lubricant containing only GO additives, (c) biological lubricant containing GO/Fol additives.

3.2.4. Lubrication Mechanism

According to the carbon structure analysis of the worn surface, the lubrication mechanism of the biological lubrication additives at the friction interface was speculated. The lubrication mechanism of the GO, Fol and GO/Fol additives on the Ti6Al4V disks is shown in Figure 8a. The uniformly dispersed lamellar GO can easily transfer into contact interfaces and form protective tribo-films during the friction process, which effectively inhibits the direct contact of the microconvex body to enhance the antiwear ability. At the same time, the lower van der Waals force between the GO nanosheets reduced the shear force of the sliding interface, which makes the interface much easier to slide and promotes friction reduction performance [27,29]. The spherical Fol can enter the contact interface of the friction pairs to separate the microconvex body and transform sliding friction into rolling friction. This means that the friction can be reduced due to the load distribution becomes uniform and the sliding shear force becomes small under the action of spherical Fol rolling at the interface [19]. Moreover, the spherical Fol could be interspersed and loaded onto the GO lamellae by hydrogen bonding when GO and Fol existed at the friction interface simultaneously, which enabled both the GO and Fol to enter the friction interface to form carbon protective tribo-films on the worn surface. Then, the rolling friction effect of Fol and the weak interlayer slip effect of GO could be exerted at the friction interface simultaneously to improve the tribological performance. In addition, some incommensurate sliding contact surfaces were formed between the GO nanosheets and spherical Fol at the interface, which further reduced the interaction forces of friction pairs [25].

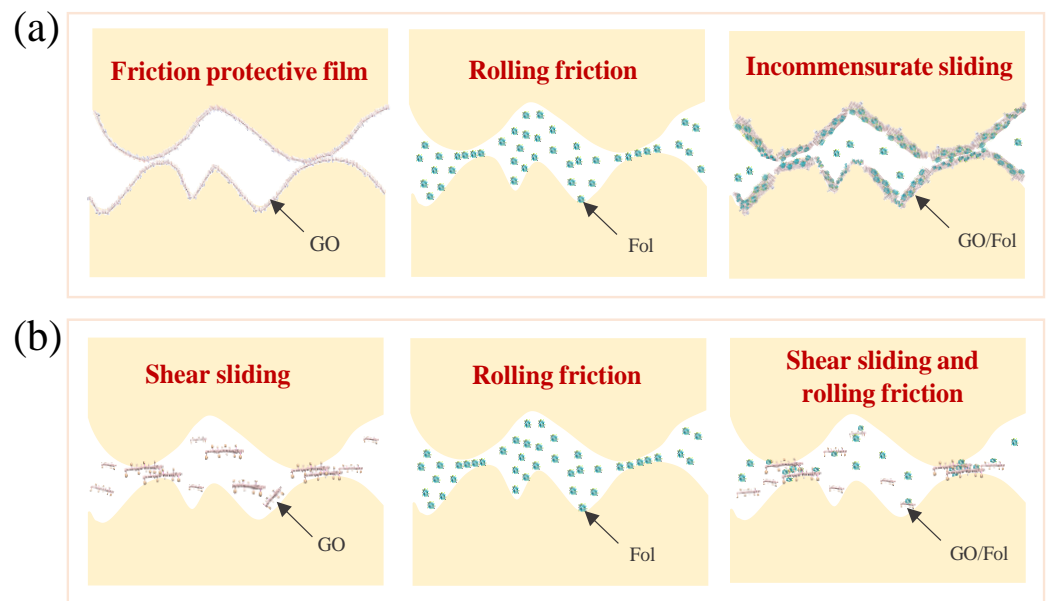


Figure 8. Lubrication mechanism of the GO, Fol and GO/Fol biological lubrication additives on (a) Ti6Al4V disks and (b) UHMWPE disks.

The lubrication mechanism of the GO, Fol and GO/Fol additives on the UHMWPE disks is shown in Figure 8b. Although GO and Fol did not easily form tribo-films on the worn surface of the UHMWPE disks, they could effectively enter the friction interface to reduce the interaction forces by the weak interlayer slip effect of GO and the rolling friction effect of Fol, respectively, to promote friction reduction performance. In addition, incommensurate sliding contact surfaces—formed between the GO nanosheets and spherical Fol at the interface—were also key to the good friction reduction performance of the GO/Fol additives on the UHMWPE disks.

3.3. Antioxidant Activity of Biological Lubrication Additives

As shown in Figure 9a,b, the free radical scavenging abilities of GO, Fol, GO/Fol = 1/1, GO/Fol = 1/2 and GO/Fol = 2/1 with different concentrations were compared. The results showed that both GO and Fol had scavenging ability on $\bullet\text{OH}$ and DPPH free radicals. The scavenging capacity was positively correlated with the concentration of the sample, which was consistent with results reported in the literature [30,31]. This is because Fol can effectively adsorb $\bullet\text{OH}$ and DPPH free radicals based on electron-deficient positions, and destroy these ROS by transferring electrons to fullerene cages (Figure 9c) [32]. At the same time, many OH groups on the surface of Fol can also remove $\bullet\text{OH}$ and DPPH free radicals by hydrogen transfer [33,34]. However, the ability of GO to scavenge free radicals is related to its SP^2 carbon structure, which plays a role through the formation of adducts or electron transfer. In addition, hydrogen atoms in oxygen-containing functional groups on the surface of GO can also participate in the neutralization of free radicals [20,35].

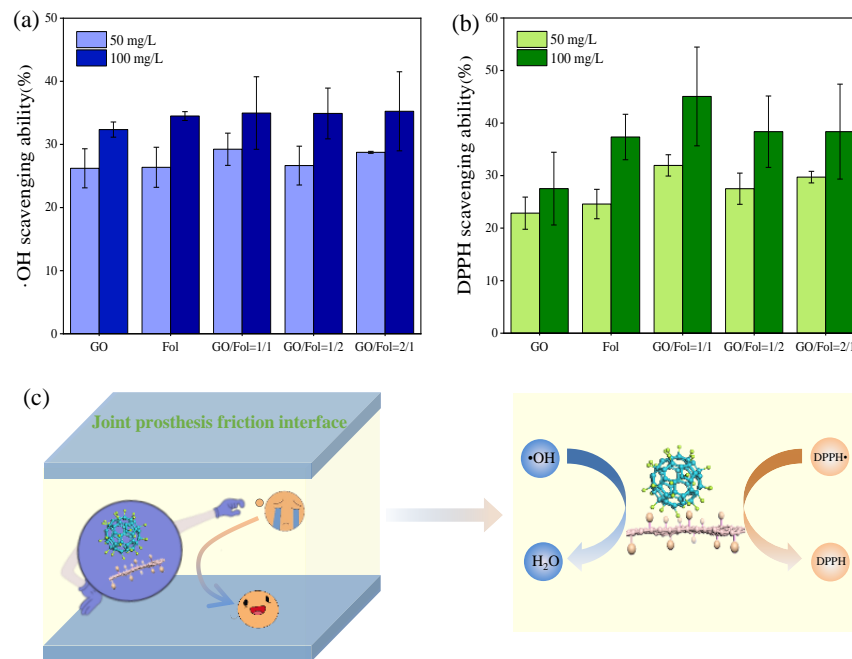


Figure 9. The (a) $\bullet\text{OH}$ and (b) DPPH free radical scavenging ability of GO, Fol and GO/Fol at different concentrations; (c) antioxidation mechanism of biological lubrication additives at joint prosthesis interface.

The scavenging ability of GO/Fol = 1/1 on $\bullet\text{OH}$ and DPPH free radicals has been improved compared with other groups, especially in the scavenging of DPPH free radical. When the concentration was 0.1 mg/mL, the scavenging effect of GO/Fol = 1/1 on $\bullet\text{OH}$ and DPPH free radicals reached 45% and 35%, respectively. The results showed that GO and Fol nanoparticles had a synergistic effect on free radical scavenging. This might be because both the spherical Fol and the lamellar GO tend to aggregate in aqueous solution to form large clusters, which would greatly reduce its ability to scavenge $\bullet\text{OH}$ and DPPH [35]. However, the spherical Fol could be interspersed and loaded onto the GO lamellae to inhibit agglomeration when GO and Fol existed in aqueous solution simultaneously, which provided more active sites for combining with free radicals and enhanced free radical scavenging ability.

4. Conclusions

In summary, GO and Fol were used as additives to prepare biological lubricants for artificial joints. The lubrication properties of biological lubricants containing different mass ratios of GO and Fol at two kinds of friction pairs were investigated comparatively. The lubrication mechanisms of GO and Fol as biological lubricant additives on the two friction pairs were revealed through the Raman characterization analysis of the friction interface. The antioxidation efficacies of the biological lubricants containing different mass ratios of GO and Fol were also evaluated. Tribological tests indicated that the synergistic effect of GO and Fol enabled the biological lubricant to exhibit superior friction reduction properties at the interface of both the Al_2O_3 -Ti6Al4V and Ti6Al4V-UHMWPE friction pairs. The average friction coefficients of the Al_2O_3 -Ti6Al4V pair and the Ti6Al4V-UHMWPE pair were reduced by 30% and 22%, respectively when GO and Fol were added to the biological lubricant with a mass ratio of 2 to 1. The superior friction reduction properties of GO and Fol can be attributed to the formation of some incommensurate sliding contact surfaces with low interfacial shear force between the GO nanosheets and spherical Fol at the friction interface. In addition, the biological lubricants containing GO and Fol also showed good antioxidant activity. The maximum scavenging rates of $\bullet\text{OH}$ and DPPH free radicals by biological lubricant containing GO and Fol were 35% and 45%, respectively. This can

be attributed to the GO and Fol scavenging free radicals through electron transfer and hydrogen transfer. All these results show that GO and Fol have good application prospects as novel biological lubricant additives for artificial joints due to their synergistic lubrication and antioxidation efficacies.

Author Contributions: Conceptualization, Q.W. and B.W.; formal analysis, Q.W. and L.W.; funding acquisition, X.H., C.L. (Chuan Li), B.W. and H.L.; investigation, Q.W., L.W. and Z.B.; methodology, C.P., C.L. (Chuanrun Li) and B.W.; writing—original draft, Q.W., Z.B., C.W. (Chao Wang) and L.C.; writing—review and editing, H.L., L.W., C.W. (Changge Wang), C.W. (Chao Wang) and L.C. All authors have read and agreed to the published version of the manuscript.

Funding: This work is funded by the Key Project of Talent Support Plan of Anhui University of Chinese Medicine (No. 2022rczd001), the National Natural Science Foundation of China (No. 52075141), the Discipline Construction Quality Improvement Project of Chaohu University (No. kj20zsys02), the Scientific Research Planning Project of Anhui Provincial (No. 2022AH010092 and No. 2022AH051726) and the Support Program for Outstanding Young Talents in Anhui Province Colleges and Universities (No. gxyq2022079).

Acknowledgments: The authors thank Enzhu Hu and Kunhong Hu of Hefei University for their assistance in the experimental tests and data analyses.

Conflicts of Interest: The authors declare no conflict of interest.

References

1. Berenbaum, F.; Wallace, I.J.; Lieberman, D.E.; Felson, D.T. Modern-day environmental factors in the pathogenesis of osteoarthritis. *Nat. Rev. Rheumatol.* **2018**, *14*, 674–681. [[CrossRef](#)] [[PubMed](#)]
2. Merola, M.; Affatato, S. Materials for hip prostheses: A review of wear and loading considerations. *Materials* **2019**, *12*, 495. [[CrossRef](#)] [[PubMed](#)]
3. Rim, Y.A.; Ju, J.H. The role of fibrosis in osteoarthritis progression. *Life* **2020**, *11*, 3. [[CrossRef](#)] [[PubMed](#)]
4. Nine, M.J.; Choudhury, D.; Hee, A.C.; Mootanah, R.; Osman, N.A.A. Wear debris characterization and corresponding biological response: Artificial hip and knee joints. *Materials* **2014**, *7*, 980–1016. [[CrossRef](#)] [[PubMed](#)]
5. Yang, F.; Tang, J.; Dai, K.; Huang, Y. Metallic wear debris collected from patients induces apoptosis in rat primary osteoblasts via reactive oxygen species-mediated mitochondrial dysfunction and endoplasmic reticulum stress. *Mol. Med. Rep.* **2019**, *19*, 1629–1637. [[CrossRef](#)] [[PubMed](#)]
6. Hameister, R.; Kaur, C.; Dheen, S.T.; Lohmann, C.H.; Singh, G. Reactive oxygen/nitrogen species (ROS/RNS) and oxidative stress in arthroplasty. *J. Biomed. Mater. Res. Part B* **2020**, *108*, 2073–2087. [[CrossRef](#)] [[PubMed](#)]
7. Zhang, X.G.; Zhang, Y.L.; Jin, Z.M. A review of the bio-tribology of medical devices. *Friction* **2022**, *10*, 4–30. [[CrossRef](#)]
8. Méndez, P.A.; Ortiz, B.L.; Vásquez, G.M.; López, B.L. Mucoadhesive chitosan/OA nanoparticles charged with celecoxib inhibit prostaglandin E 2 LPS-induced in U 937 cell line. *J. Appl. Polym. Sci.* **2017**, *134*, 45288. [[CrossRef](#)]
9. Everhart, J.S.; DiBartola, A.C.; Swank, K.; Pettit, R.; Hughes, L.; Lewis, C.; Flanagan, D.C. Cartilage damage at the time of anterior cruciate ligament reconstruction is associated with weaker quadriceps function and lower risk of future ACL injury. *Knee Surg. Sport. Traumatol. Arthrosc.* **2020**, *28*, 576–583. [[CrossRef](#)]
10. Gleghorn, J.P.; Bonassar, L.J. Lubrication mode analysis of articular cartilage using Stribeck surfaces. *J. Biomech.* **2008**, *41*, 1910–1918. [[CrossRef](#)]
11. Huang, H.; Lou, Z.; Zheng, S.; Wu, J.; Yao, Q.; Chen, R.; Kou, L.; Chen, D. Intra-articular drug delivery systems for osteoarthritis therapy: Shifting from sustained release to enhancing penetration into cartilage. *Drug Deliv.* **2022**, *29*, 767–791. [[CrossRef](#)]
12. Šimek, M.; Nešporová, K.; Kocurková, A.; Foglová, T.; Ambrožová, G.; Velebný, V.; Kubala, L.; Hermannová, M. How the molecular weight affects the in vivo fate of exogenous hyaluronan delivered intravenously: A stable-isotope labelling strategy. *Carbohydr. Polym.* **2021**, *263*, 117927. [[CrossRef](#)] [[PubMed](#)]
13. Li, C.; Wu, B.; Chen, X.; Li, L.; Wang, X.; Gao, X.; Wang, X.; Hu, K.; Hu, X. Synergistic Lubricating Performance of Graphene Oxide and Modified Biodiesel Soot as Water Additives. *Lubricants* **2022**, *10*, 175. [[CrossRef](#)]
14. Song, H.-J.; Li, N. Frictional behavior of oxide graphene nanosheets as water-base lubricant additive. *Appl. Phys. A* **2011**, *105*, 827–832. [[CrossRef](#)]
15. Sarno, M.; Senatore, A.; Cirillo, C.; Petrone, V.; Ciambelli, P. Oil lubricant tribological behaviour improvement through dispersion of few layer graphene oxide. *J. Nanosci. Nanotechnol.* **2014**, *14*, 4960–4968. [[CrossRef](#)]
16. Zhao, J.; Mao, J.; Li, Y.; He, Y.; Luo, J. Friction-induced nano-structural evolution of graphene as a lubrication additive. *Appl. Surf. Sci.* **2018**, *434*, 21–27. [[CrossRef](#)]
17. Chen, Z.; Liu, Y.; Luo, J. Tribological properties of few-layer graphene oxide sheets as oil-based lubricant additives. *Chin. J. Mech. Eng.* **2016**, *29*, 439–444. [[CrossRef](#)]

18. Liu, Y.; Wang, X.; Liu, P.; Zheng, J.; Shu, C.; Pan, G.; Luo, J. Modification on the tribological properties of ceramics lubricated by water using fullerene as a lubricating additive. *Sci. China Technol. Sci.* **2012**, *55*, 2656–2661. [[CrossRef](#)]
19. Chen, S.; Ding, Q.; Gu, Y.; Quan, X.; Ma, Y.; Jia, Y.; Xie, H.; Tang, J. Study of tribological properties of fullerene and nanodiamonds as additives in water-based lubricants for amorphous carbon (aC) coatings. *Nanomaterials* **2021**, *12*, 139. [[CrossRef](#)]
20. Zhou, Y.; Li, J.; Ma, H.; Zhen, M.; Guo, J.; Wang, L.; Jiang, L.; Shu, C.; Wang, C. Biocompatible [60]/[70] Fullerenes: Potent defense against oxidative injury induced by reduplicative chemotherapy. *ACS Appl. Mater. Interfaces* **2017**, *9*, 35539–35547. [[CrossRef](#)]
21. Voitko, K.V.; Goshovska, Y.V.; Demianenko, E.M.; Sementsov, Y.I.; Zhuravskiy, S.V.; Mys, L.A.; Korkach, Y.P.; Kolev, H.; Sagach, V.F. Graphene oxide nanoflakes prevent reperfusion injury of Langendorff isolated rat heart providing antioxidative activity in situ. *Free Radical Res.* **2022**, *56*, 328–341. [[CrossRef](#)] [[PubMed](#)]
22. Halenova, T.; Raksha, N.; Vovk, T.; Savchuk, O.; Ostapchenko, L.; Prylutskiy, Y.; Kyzyma, O.; Ritter, U.; Scharff, P. Effect of C60 fullerene nanoparticles on the diet-induced obesity in rats. *Int. J. Obes.* **2018**, *42*, 1987–1998. [[CrossRef](#)] [[PubMed](#)]
23. Forman, H.J.; Zhang, H. Targeting oxidative stress in disease: Promise and limitations of antioxidant therapy. *Nat. Rev. Drug Discov.* **2021**, *20*, 689–709. [[CrossRef](#)] [[PubMed](#)]
24. Goodarzi, S.; Da Ros, T.; Conde, J.; Sefat, F.; Mozafari, M. Fullerene: Biomedical engineers get to revisit an old friend. *Mater. Today* **2017**, *20*, 460–480. [[CrossRef](#)]
25. Wu, B.; Song, H.; Zhang, Q.; Hu, X. Controllable synthesis and friction reduction of ZnFe₂O₄@C microspheres with diverse core-shell architectures. *Tribol. Int.* **2021**, *153*, 106614. [[CrossRef](#)]
26. Jaiswal, R.; Saha, U.; Goswami, T.H.; Srivastava, A.; Prasad, N.E. ‘Pillar effect’ of chemically bonded fullerene in enhancing supercapacitance performances of partially reduced fullerene/graphene oxide hybrid electrode material. *Electrochim. Acta* **2018**, *283*, 269–290. [[CrossRef](#)]
27. Xie, H.; Jiang, B.; Dai, J.; Peng, C.; Li, C.; Li, Q.; Pan, F. Tribological behaviors of graphene and graphene oxide as water-based lubricant additives for magnesium alloy/steel contacts. *Materials* **2018**, *11*, 206. [[CrossRef](#)]
28. Su, F.; Chen, G.; Huang, P. Lubricating performances of graphene oxide and onion-like carbon as water-based lubricant additives for smooth and sand-blasted steel discs. *Friction* **2020**, *8*, 47–57. [[CrossRef](#)]
29. Song, H.; Wang, Z.; Yang, J. Tribological properties of graphene oxide and carbon spheres as lubricating additives. *Appl. Phys. A.* **2016**, *122*, 933. [[CrossRef](#)]
30. Hao, T.; Li, J.; Yao, F.; Dong, D.; Wang, Y.; Yang, B.; Wang, C. Injectable fullerene/alginate hydrogel for suppression of oxidative stress damage in brown adipose-derived stem cells and cardiac repair. *ACS Nano* **2017**, *11*, 5474–5488. [[CrossRef](#)]
31. Abdelhalim, A.O.; Meshcheriakov, A.A.; Maistrenko, D.N.; Molchanov, O.E.; Ageev, S.V.; Ivanova, D.A.; Iamalova, N.R.; Luttsev, M.D.; Vasina, L.V.; Sharoyko, V.V. Graphene oxide enriched with oxygen-containing groups: On the way to an increase of antioxidant activity and biocompatibility. *Colloids Surf. B* **2022**, *210*, 112232. [[CrossRef](#)] [[PubMed](#)]
32. Wang, J.; Hu, Z.; Xu, J.; Zhao, Y. Therapeutic applications of low-toxicity spherical nanocarbon materials. *NPG Asia Mater.* **2014**, *6*, e84. [[CrossRef](#)]
33. Wang, Z.; Gao, X.; Zhao, Y. Mechanisms of antioxidant activities of fullerenols from first-principles calculation. *J. Phys. Chem. A* **2018**, *122*, 8183–8190. [[CrossRef](#)] [[PubMed](#)]
34. Podolsky, N.E.; Marcos, M.A.; Cabaleiro, D.; Semenov, K.N.; Lugo, L.; Petrov, A.V.; Charykov, N.A.; Sharoyko, V.V.; Vlasov, T.D.; Murin, I.V. Physico-chemical properties of C60 (OH) 22–24 water solutions: Density, viscosity, refraction index, isobaric heat capacity and antioxidant activity. *J. Mol. Liq.* **2019**, *278*, 342–355. [[CrossRef](#)]
35. Awan, F.; Bulger, E.; Berry, R.M.; Tam, K.C. Enhanced radical scavenging activity of polyhydroxylated C60 functionalized cellulose nanocrystals. *Cellulose* **2016**, *23*, 3589–3599. [[CrossRef](#)]

Disclaimer/Publisher’s Note: The statements, opinions and data contained in all publications are solely those of the individual author(s) and contributor(s) and not of MDPI and/or the editor(s). MDPI and/or the editor(s) disclaim responsibility for any injury to people or property resulting from any ideas, methods, instructions or products referred to in the content.